

Supporting Information

Insight into the Ordering Process and Ethanol Oxidation

Performance of Au-Pt-Cu Ternary Alloys

Wenbo Zhao,[†] Mengyao Li,[†] Shi Hu^{†*}

[†]Department of Chemistry, School of Science, Tianjin Key Laboratory of Molecular Optoelectronic Science, Tianjin University, Tianjin 300072, China.

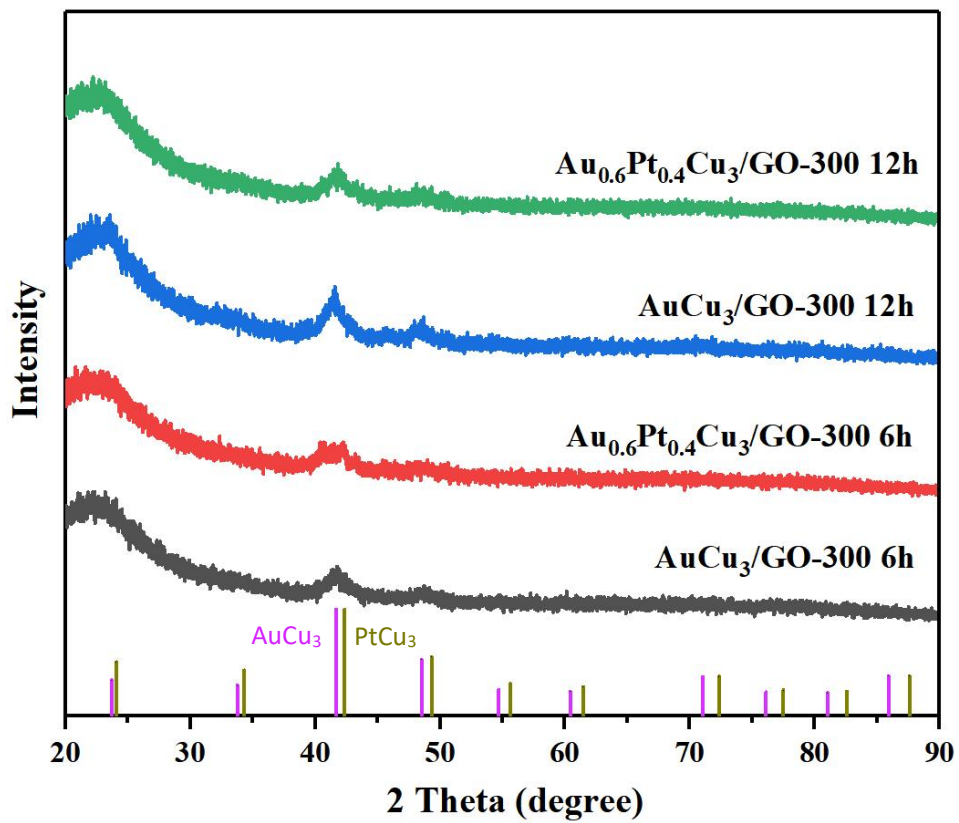


Fig. S1 The synthesis of $\text{Au}_x\text{Pt}_{1-x}\text{Cu}_3/\text{rGO}$ under 300 degrees.

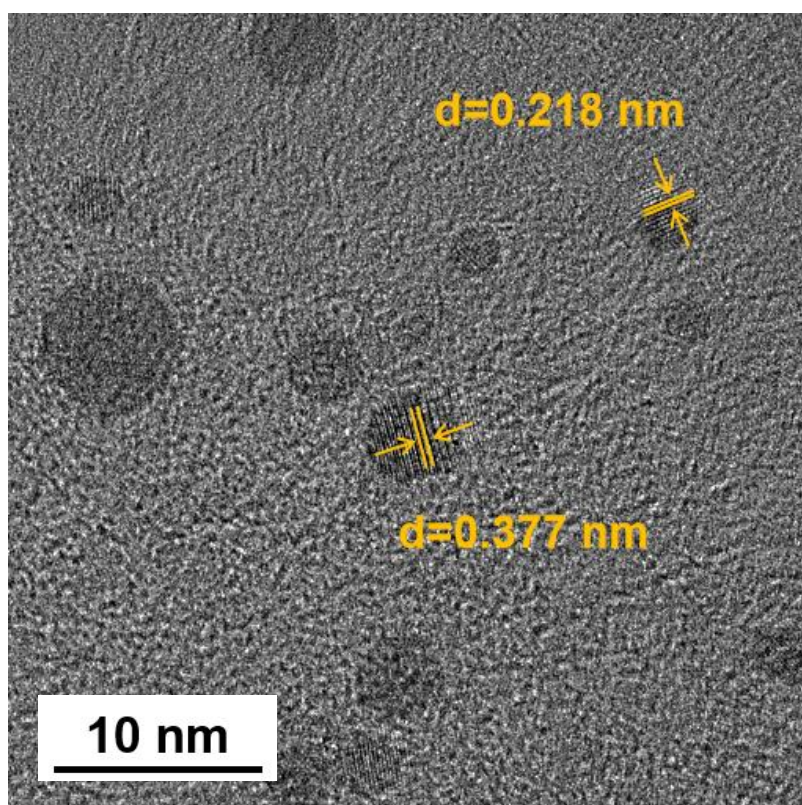
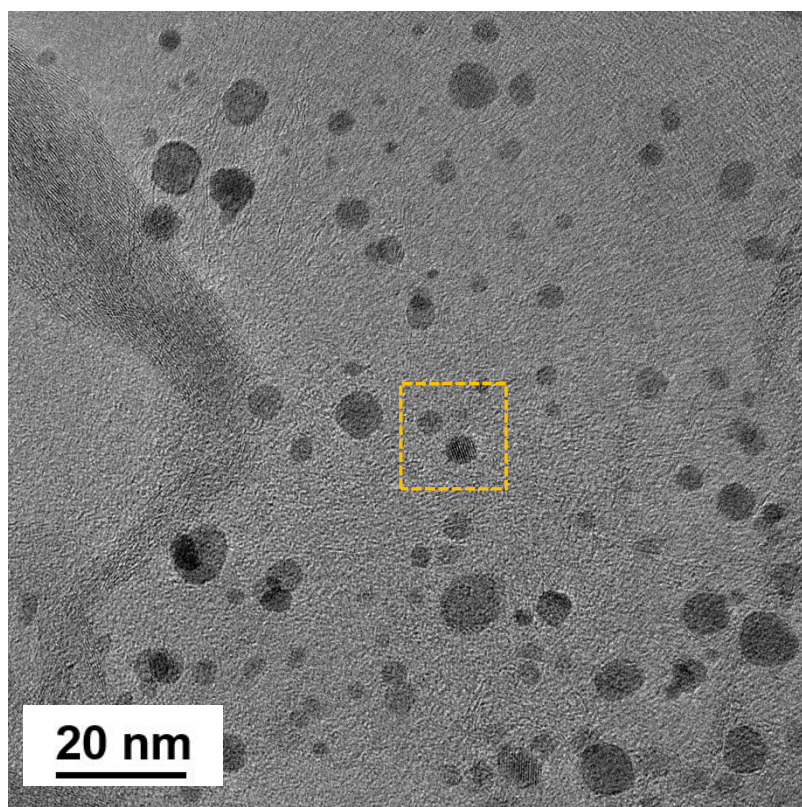


Fig. S2 High-resolution transmission electron microscopy images of $\text{Au}_{0.2}\text{Pt}_{0.8}\text{Cu}_3/\text{rGO}$.

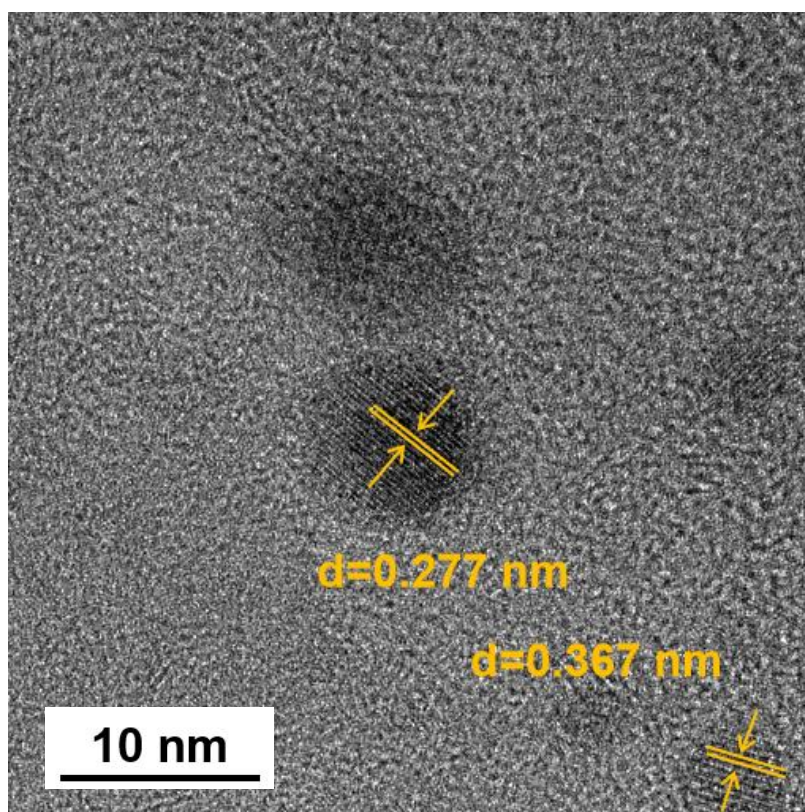
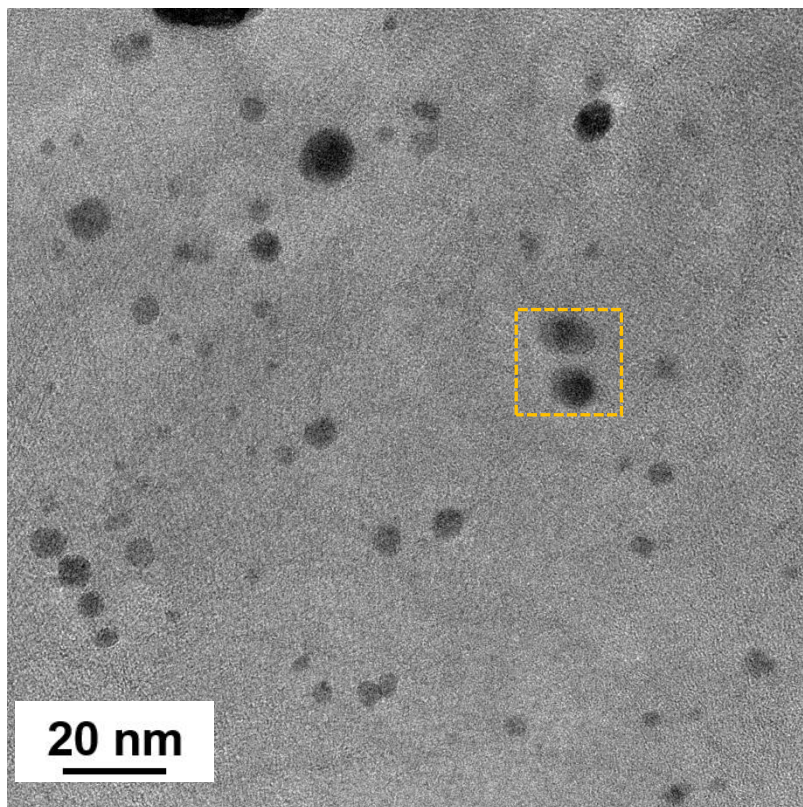


Fig. S3 High-resolution transmission electron microscopy images of $\text{Au}_{0.6}\text{Pt}_{0.4}\text{Cu}_3/\text{rGO}$.

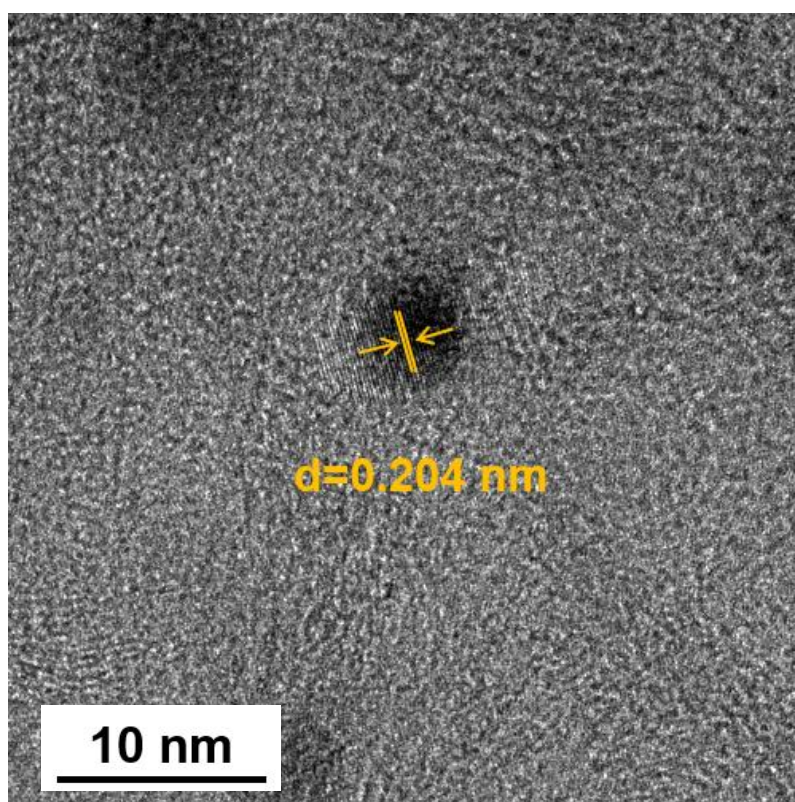
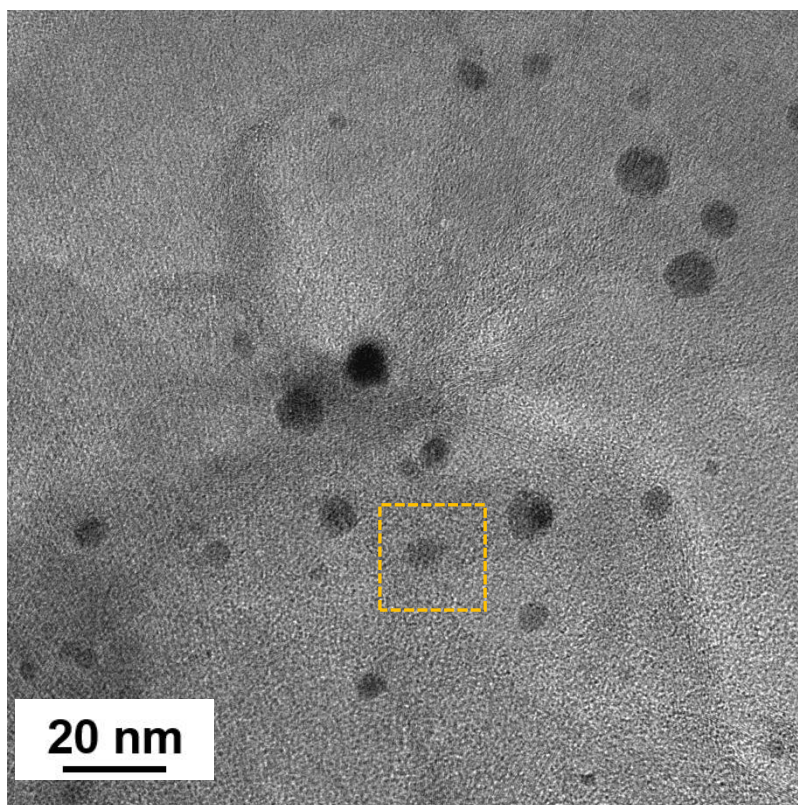


Fig. S4 High-resolution transmission electron microscopy images of $\text{Au}_{0.8}\text{Pt}_{0.2}\text{Cu}_3/\text{rGO}$.

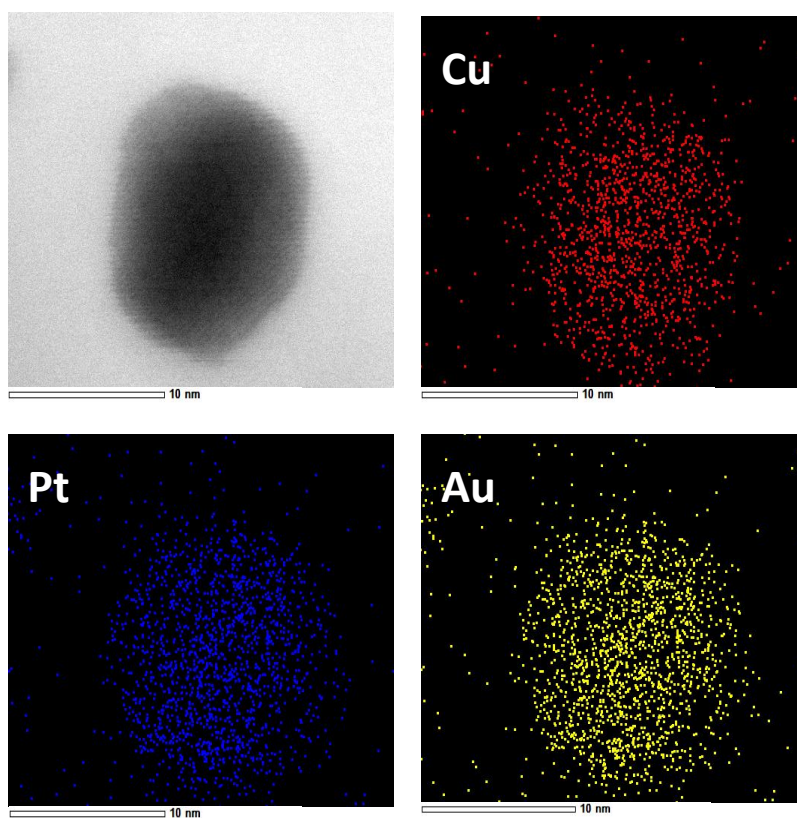


Fig. S5 Energy Dispersive Spectroscopy (EDS) mapping of $\text{Au}_{0.2}\text{Pt}_{0.8}\text{Cu}_3/\text{rGO}$.

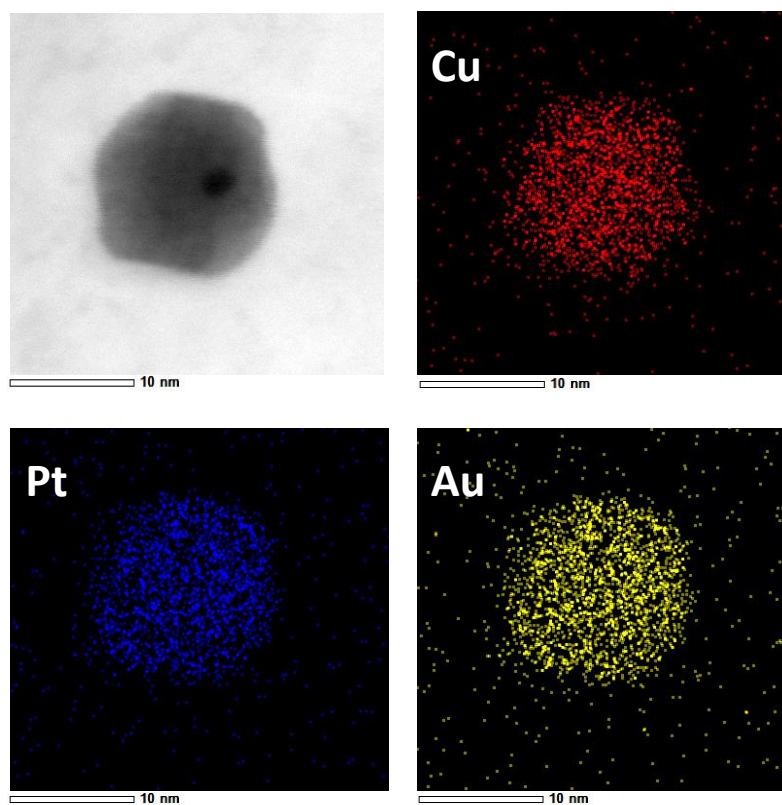


Fig. S6 Energy Dispersive Spectroscopy (EDS) mapping of $\text{Au}_{0.6}\text{Pt}_{0.4}\text{Cu}_3/\text{rGO}$.

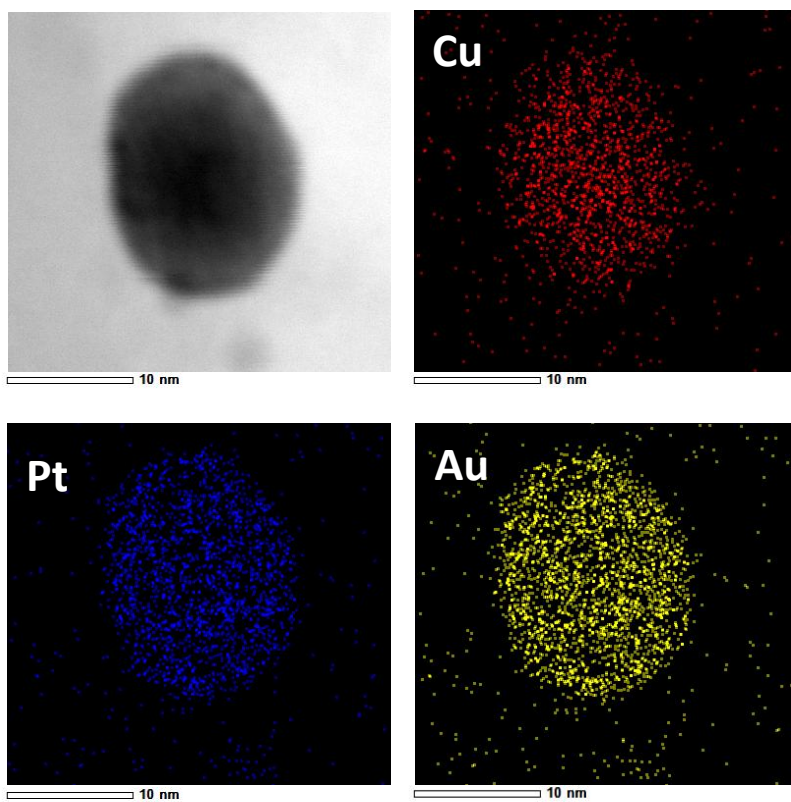


Fig. S7 Energy Dispersive Spectroscopy (EDS) mapping of $\text{Au}_{0.8}\text{Pt}_{0.2}\text{Cu}_3/\text{rGO}$.

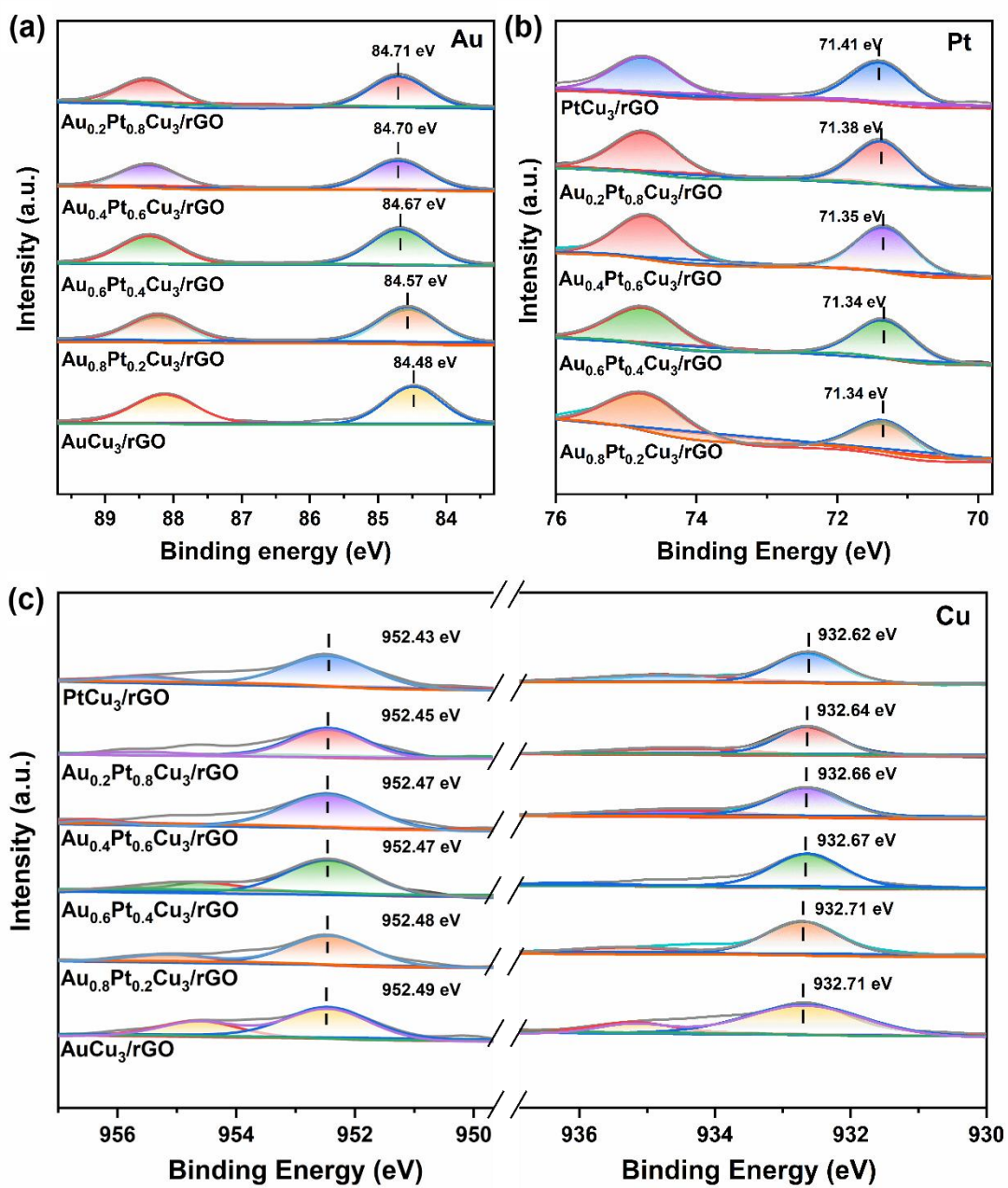


Fig. S8 X-ray photoelectron spectroscopy patterns of (a) Au 4f, (b) Pt 4f, (c) Cu 2p_{1/2} and Cu 2p_{3/2} in Au_xPt_{1-x}Cu₃/rGO ordered alloys.

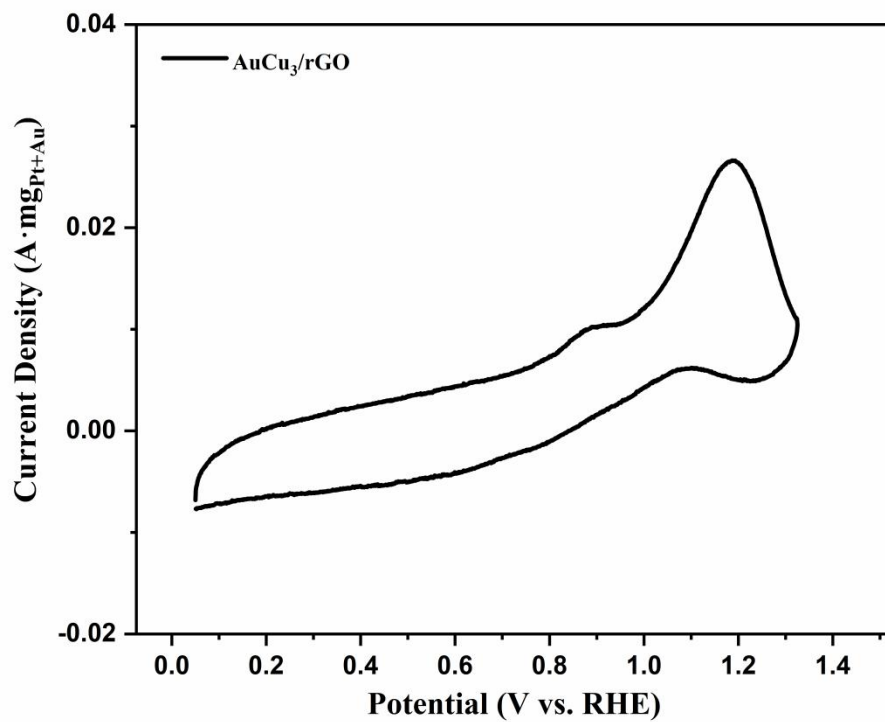


Fig. S9 Ethanol oxidation reaction in 1.0 M KOH and 1.0M EtOH with AuCu₃/rGO.

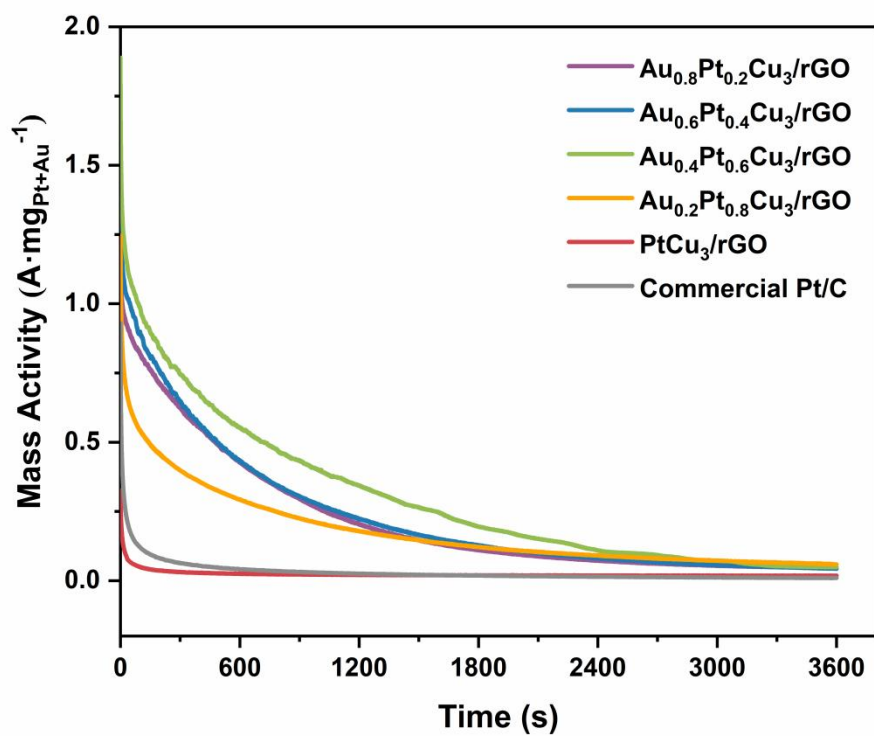


Fig. S10 Chronoamperometry testing at 0.77 V_{RHE} for 3600 seconds in N₂-saturated 1.0 M KOH and 1.0 M EtOH mixture solution.

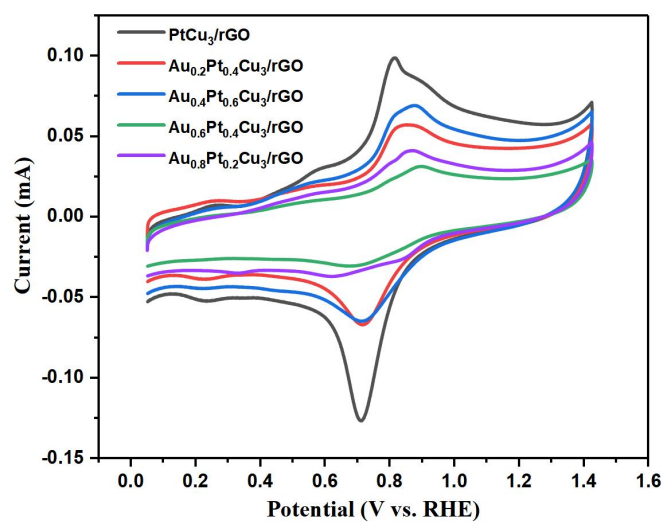


Fig. S11 Cyclic Voltammetry of Au_xPt_{1-x}Cu₃/rGO in 1.0M KOH with a scan rate of 50 mV • s⁻¹..

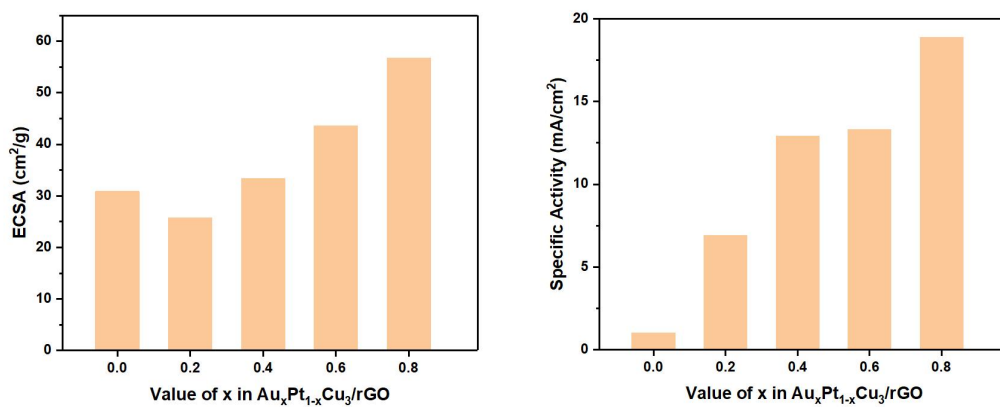


Fig. S12 Electrochemical active surface area (ECSA) and specific activity of Au_xPt_{1-x}Cu₃/rGO in 1.0 M KOH and 1.0M EtOH. The ECSA is calculated with the area of the Pt oxide reduction peak.¹⁻²

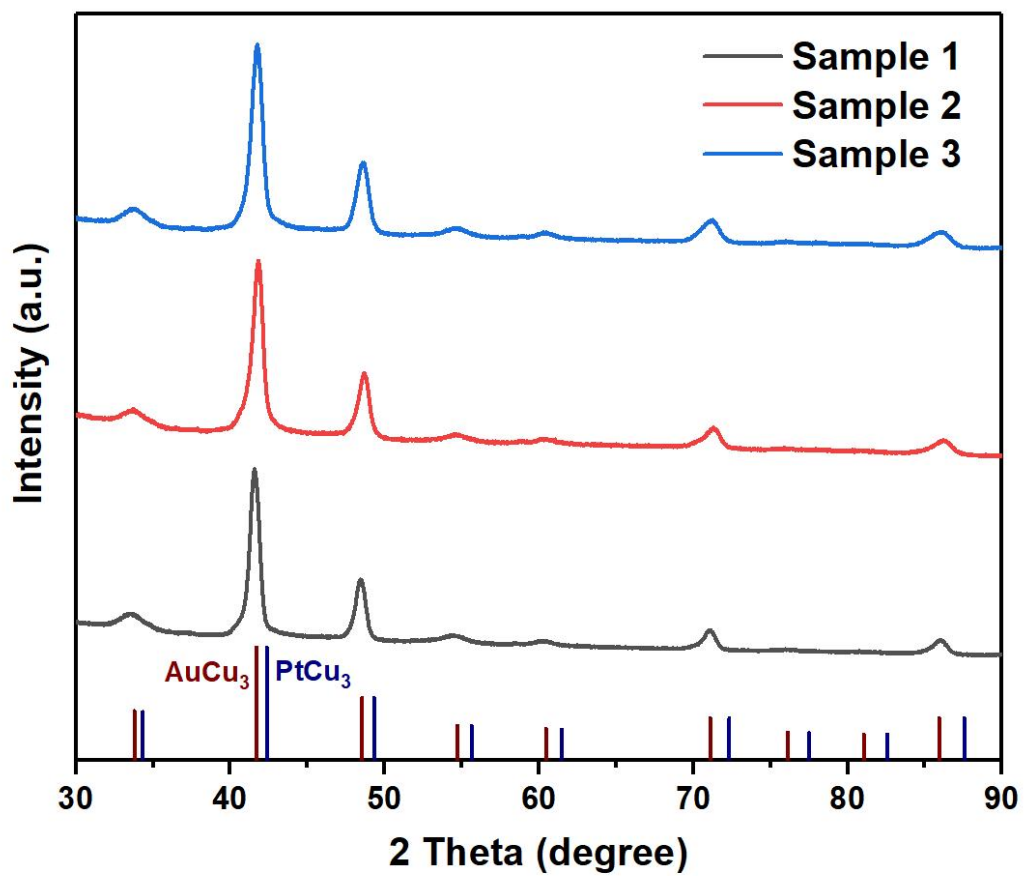


Fig. S13 XRD pattern of AuCu₃/rGO parallel samples.

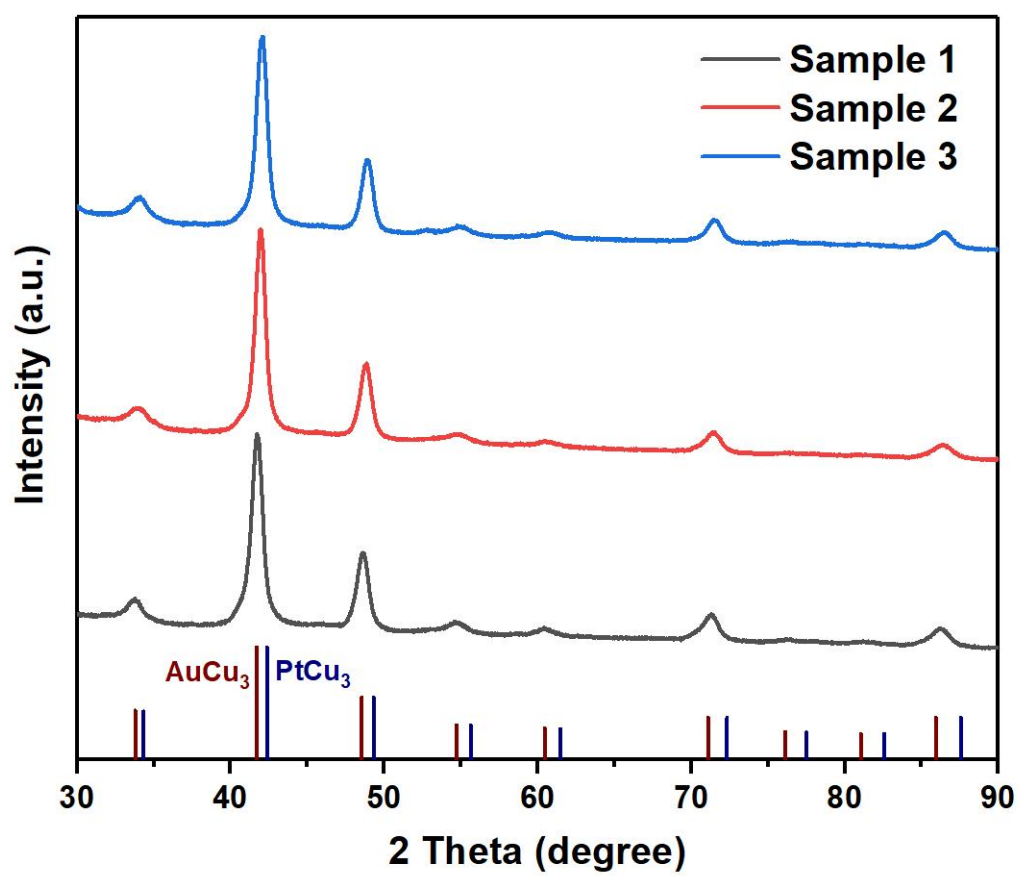


Fig. S14 XRD pattern of Au_{0.8}Pt_{0.2}Cu₃/rGO parallel samples.

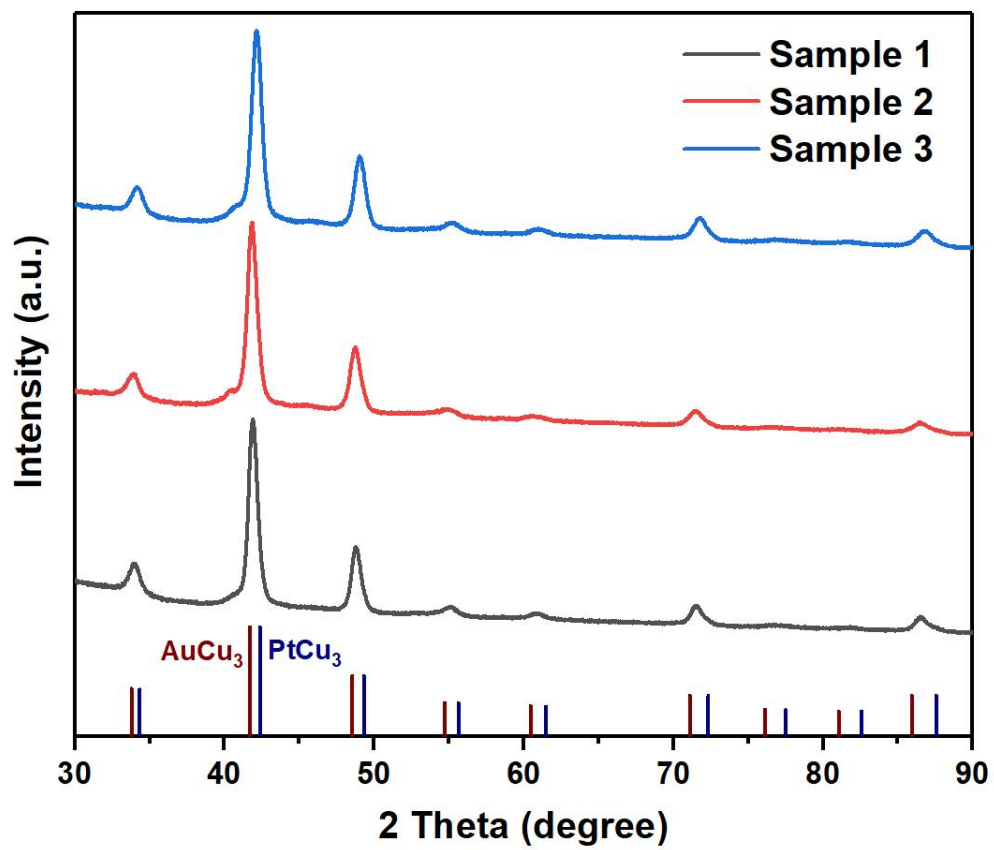


Fig. S15 XRD pattern of Au_{0.6}Pt_{0.4}Cu₃/rGO parallel samples.

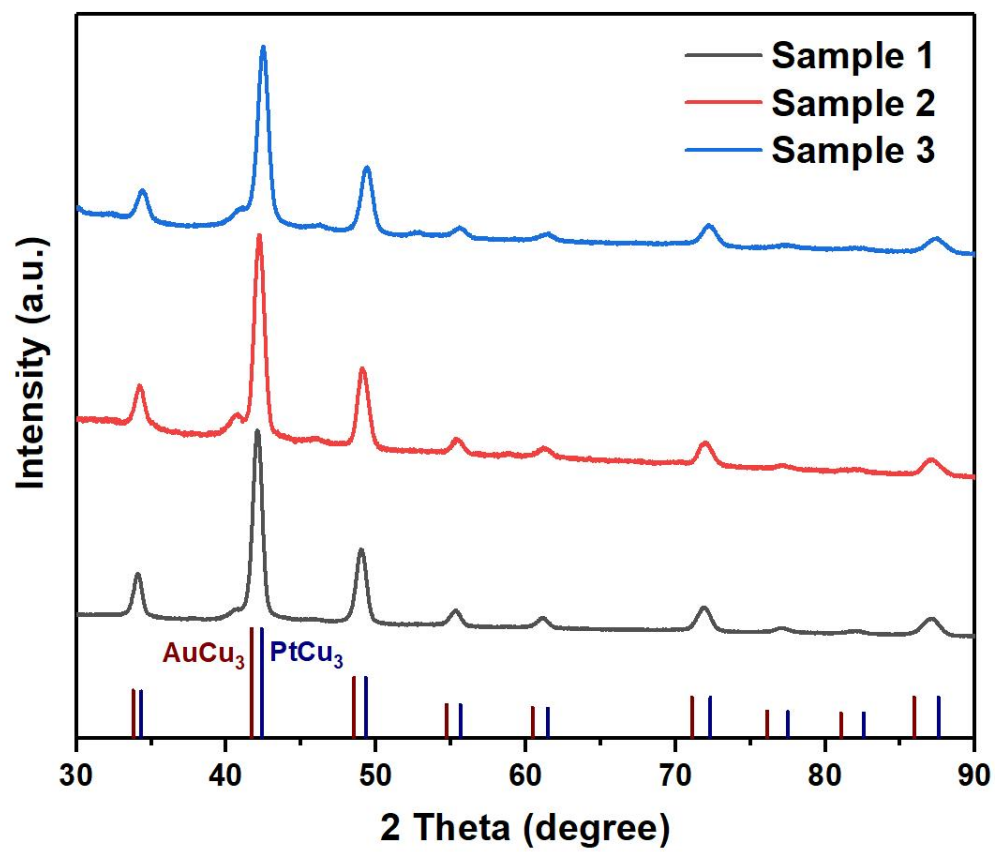


Fig. S16 XRD pattern of $\text{Au}_{0.4}\text{Pt}_{0.6}\text{Cu}_3/\text{rGO}$ parallel samples.

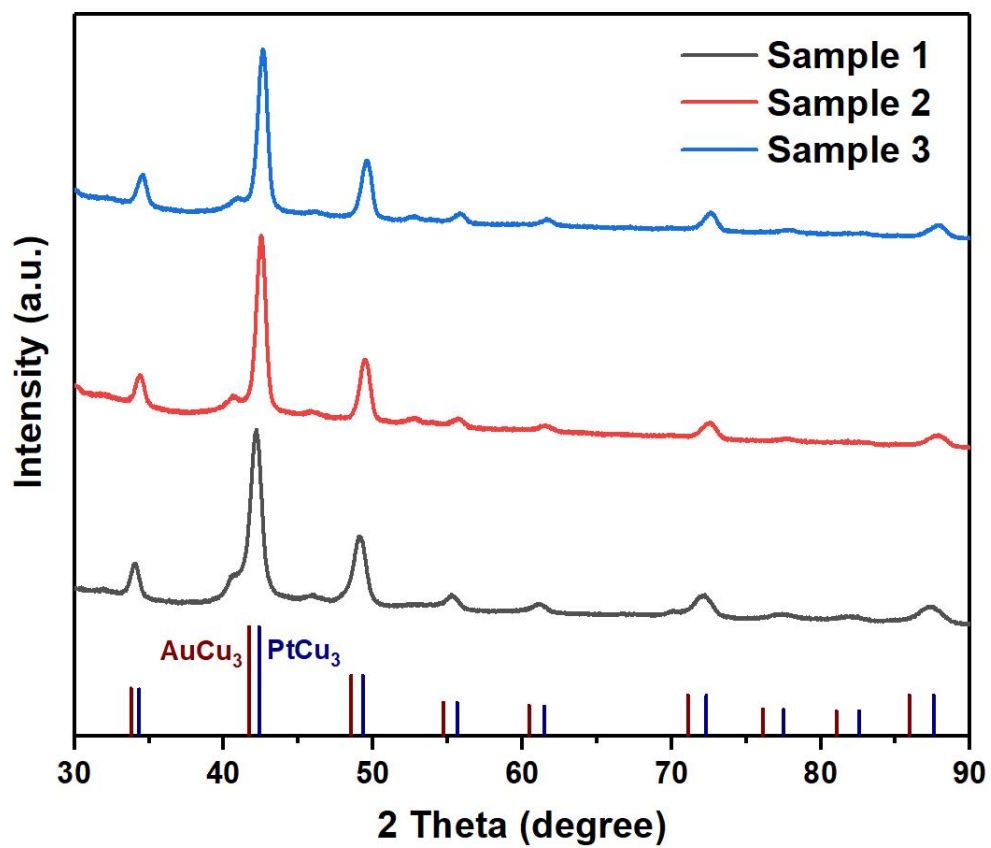


Fig. S17 XRD pattern of $\text{Au}_{0.2}\text{Pt}_{0.8}\text{Cu}_3/\text{rGO}$ parallel samples.

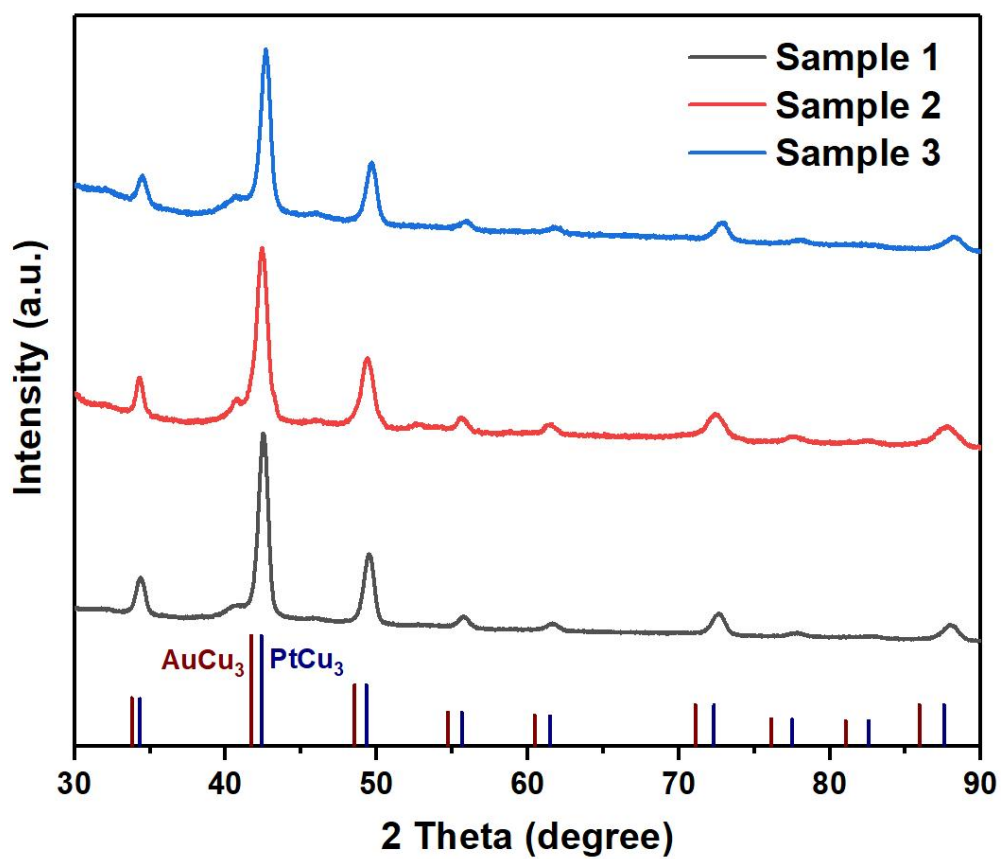


Fig. S18 XRD pattern of PtCu₃/rGO parallel samples.

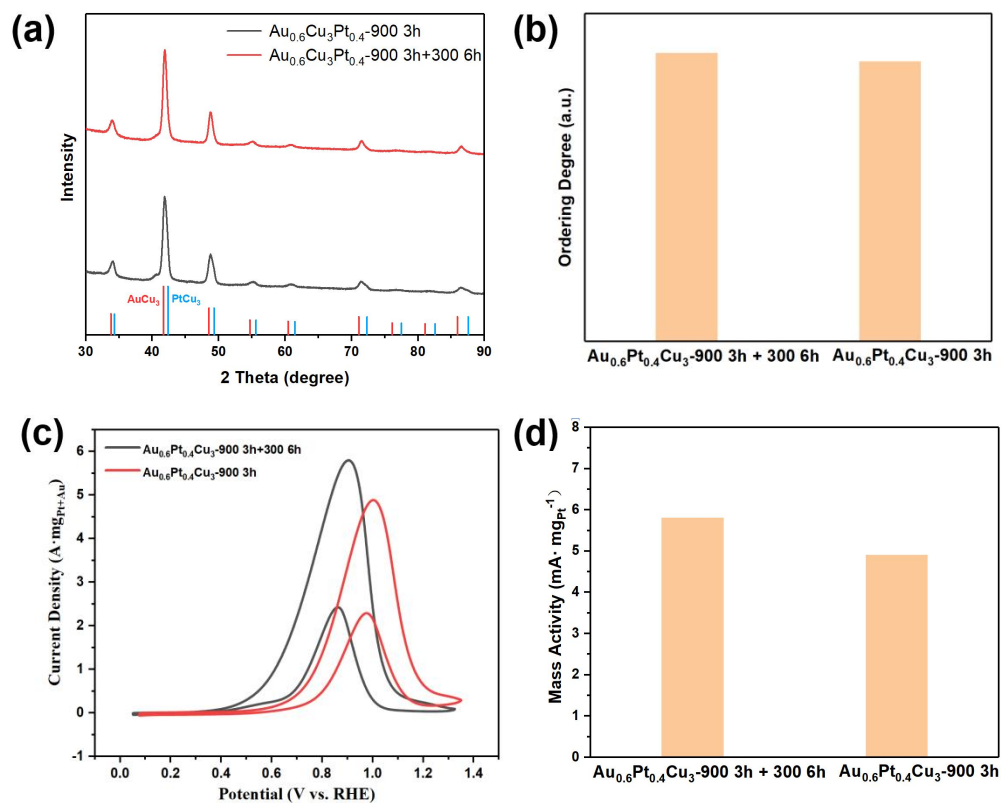


Fig. S19 (a) XRD pattern of $\text{Au}_{0.6}\text{Pt}_{0.4}\text{Cu}_3/\text{rGO}$ samples annealed at 900°C for 3h, annealed at 900°C for 3h and 300°C for 6h and (b) their ordering degree. (c) Ethanol oxidation performance of $\text{Au}_{0.6}\text{Pt}_{0.4}\text{Cu}_3/\text{rGO}$ samples annealed at 900°C for 3h, annealed at 900°C for 3h and 300°C for 6h and (d) activity comparison.

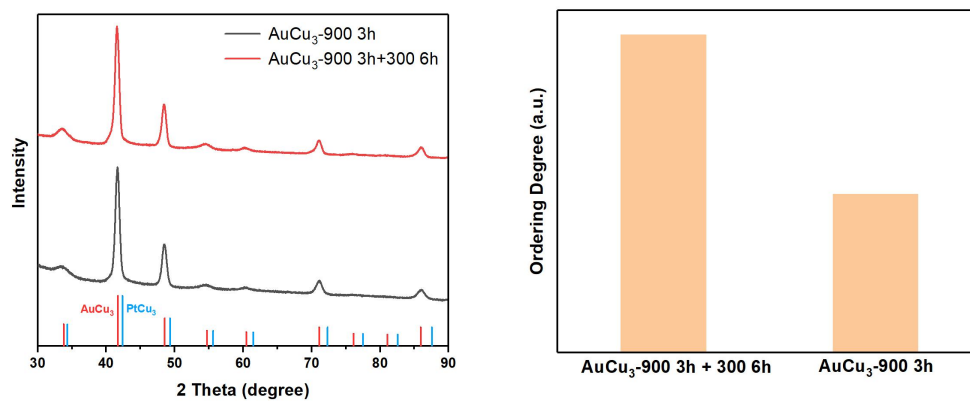


Fig. S20 XRD pattern of AuCu₃/rGO samples annealed at 900°C for 3h, annealed at 900°C for 3h and 300°C for 6h and their ordering degree.

Table S1 ICP results of Au_xPt_{1-x}Cu₃/rGO samples with various values of x.

Sample	Atomic Ratio		
	Au	Cu	Pt
PtCu ₃ /rGO	0	0.818607955	0.181392045
Au _{0.2} Cu ₃ Pt _{0.8} /rGO	0.028962411	0.829645331	0.141392258
Au _{0.4} Cu ₃ Pt _{0.6} /rGO	0.073480344	0.823508243	0.103011414
Au _{0.6} Cu ₃ Pt _{0.4} /rGO	0.115593784	0.81551273	0.068893487
Au _{0.8} Cu ₃ Pt _{0.2} /rGO	0.138738842	0.826128833	0.035132325
AuCu ₃ /rGO	0.217636877	0.782363123	0

Table S2 Ratios of precursors in Au_xPt_{1-x}Cu₃/rGO samples with various values of x.

Sample	HAuCl ₄ ·4H ₂ O (mmol)	CuCl ₂ ·2H ₂ O (mmol)	H ₂ PtCl ₆ ·6H ₂ O (mmol)
PtCu ₃ /rGO	0	0.075	0.025
Au _{0.2} Cu ₃ Pt _{0.8} /rGO	0.005	0.075	0.020
Au _{0.4} Cu ₃ Pt _{0.6} /rGO	0.010	0.075	0.015
Au _{0.6} Cu ₃ Pt _{0.4} /rGO	0.015	0.075	0.010
Au _{0.8} Cu ₃ Pt _{0.2} /rGO	0.020	0.075	0.005
AuCu ₃ /rGO	0.025	0.075	0

Table S3 d-band center of Pt in the Pt₁₈Cu₅₄.

Sites	d-band center (eV)
Pt1:	-1.9396
Pt2:	-1.9422
Pt3:	-1.9428
Pt4:	-1.9423
Pt5:	-1.9409
Pt6:	-1.9421
Pt7:	-1.9436
Pt8:	-1.941
Pt9:	-1.9411
Pt10:	-1.9395
Pt11:	-1.9425
Pt12:	-1.9427
Pt13:	-1.9421
Pt14:	-1.9409
Pt15:	-1.9421
Pt16:	-1.9433
Pt17:	-1.9411
Pt18:	-1.9403
Average	-1.9417

Table S4 d-band center of Pt in the Au₆Pt₁₂Cu₅₄.

Sites	d-band center (eV)
Pt1:	-1.9841
Pt2:	-2.0016
Pt3:	-2.003
Pt4:	-1.9831
Pt5:	-1.9941
Pt6:	-1.9945
Pt7:	-1.9814
Pt8:	-1.9871
Pt9:	-1.987
Pt10:	-1.9813
Pt11:	-1.977
Pt12:	-1.9776
Average	-1.98765

Table S5 d-band center of Pt in the Au₁₂Pt₆Cu₅₄.

Sites	d-band center (eV)
Pt1:	-2.1428
Pt2:	-2.1434
Pt3:	-2.1096
Pt4:	-2.1625
Pt5:	-2.1505
Pt6:	-2.1428
Average	-2.1419

Reference

- (1) F. P. Lohmann-Richters, B. Abel and Á. Varga, *J. Mater. Chem. A*, 2018, 6, 2700-2707.
- (2) M. Łukaszewski, M. Soszko and A. Czerwiński, *Int. J. Electrochem. Sci.*, 2016, 11, 4442-4469.